

$\epsilon_r = 12$ ) and X band (0.63 mm and 0.38 mm, and  $\epsilon_r = 12$ ). Typical results for an X-band coupler, including the connectors, are shown in Fig. 13. When measuring the isolation, i.e.,  $|A_3|^2$  the effect of unwanted reflections from connectors has been reduced by putting absorbing material on the strips of the arms 2 and 4. Similar results but with total losses of about 0.3 dB have been obtained for C band. The strength of the coupling can be increased continuously (by about 1 dB) by loading the slot with dielectric materials of different thickness. The coupler performance was reproducible from sample to sample within a few tenths of a decibel and no correction in the design was necessary. No change in the coupler performance was noticed and no resonances occurred when a shielding box was used, leading to the conclusion that radiation loss is negligible. A balanced mixer made with such a coupler had a very constant noise figure of about 9–9.5 dB from 7–12.4 GHz.

Also an octave wide C-band matched leveller with two p-i-n diodes was built around this coupler with about 1-dB insertion loss and a minimum of 15-dB variable attenuation.

The slot-strip-slot-type coupler (Fig. 6) has also been realized in C band with a geometry similar to Fig. 4 but with slot and strip interchanged. With a slot width of 40  $\mu\text{m}$  after etching and a dielectric loading, a coupling of 4 dB was obtained. The bandwidth was somewhat lower than for the de Ronde type of coupler and additional work is needed to optimize also the slot-strip-slot coupler.

## VI. CONCLUSION

The hybrid branchline couplers with series and shunt branches are analyzed and shown to form a class of useful couplers, to which also the transmission-line coupler and de Ronde's strip-slot coupler belong. From the precise design data now available, a number of strip-slot 3-dB couplers have been built and their relevant parameters were close to the predicted ones.

## ACKNOWLEDGMENT

The author wishes to thank W. Schilz, M. Lemke, J. Köhler, and F. C. de Ronde for valuable comments and discussions, and Mrs. H. Runge for help with the measurements and the numerical calculations.

## REFERENCES

- [1] J. Lange, "Interdigitated strip-line quadrature hybrid," in *1969 G-MTT Int. Microwave Symp.*, pp. 10–13.
- [2] L. Young, "Parallel coupled lines and directional couplers," in *ARTECH House Reprint Volume*. Dedham, Mass.: ARTECH.
- [3] F. C. de Ronde, "A new class of microstrip directional couplers," in *1970 IEEE Int. Microwave Symp.*, May 1970, pp. 184–186.
- [4] J. A. Garcia, "A wide-band quadrature hybrid coupler," *Trans. Microwave Theory Tech. (Special Issue on Microwave Integrated Circuits)*, vol. MTT-19, pp. 660–661, July 1971.
- [5] J. Reed and G. J. Wheeler, "A method of analysis of symmetrical four-port networks," *IRE Trans. Microwave Theory Tech. (Special Issue on the National Symposium on Microwave Techniques)*, vol. MTT-4, pp. 246–252, Oct. 1956.
- [6] E. M. T. Jones and J. T. Bolljahn, "Coupled-strip-transmission-line filters and directional couplers," *IRE Trans. Microwave Theory Tech.*, vol. MTT-4, pp. 75–81, Apr. 1956.
- [7] S. B. Cohn, "Slot line on a dielectric substrate," *IEEE Trans. Microwave Theory Tech.*, vol. MTT-17, pp. 768–778, Oct. 1969.

# The Design of a Bandpass Filter with Inductive Strip—Planar Circuit Mounted in Waveguide

YOSHIHIRO KONISHI, SENIOR MEMBER, IEEE, AND KATSUAKI UENAKADA, MEMBER, IEEE

**Abstract**—The equivalent circuit of an inductive strip inserted in the middle of a waveguide parallel to the  $E$  plane is analyzed theoretically by evaluating the inductive reactance of the equivalent  $T$  network which was obtained by the Rayleigh-Ritz variational technique. A design theory for the bandpass filter of this type is derived from this equivalent circuit. The confirmation between the design theory and the experimental results is also shown.

Manuscript received January 22, 1974; revised April 17, 1974.  
The authors are with the Technical Research Laboratories, Nippon Hoso Kyokai, Japan Broadcasting Corporation, Tokyo, Japan.

## INTRODUCTION

**F**ILTERS using conventional inductive elements such as rods, transverse strips, and transverse diaphragms are difficult to make low cost and to put into mass production because of their complicated structure. To solve this problem, microstrip circuits have been used. However, these, typically, are lossy. Therefore, we have developed a circuit consisting of a metal sheet with appropriate patterns that is inserted in the middle of a waveguide

parallel to the  $E$  plane. A simplified 12-GHz low-noise converter using this circuit was reported [1]. This planar circuit is very useful for low-cost mass production and has an unloaded  $Q$  factor of 2000–2500 at  $X$  band. The accuracy of the patterns for the filter is maintained within  $20 \mu\text{m}$  with a 0.5-mm-thick sheet by using pressing techniques.

In this paper, a design theory for the planar circuit bandpass filter with inductive strip is presented. First, the equivalent  $T$  network of an inductive strip inserted in the middle of the waveguide parallel to the  $E$  plane is represented. The equivalent circuit of the inductive strip is calculated using a variational technique under the assumption of the perfectly conductive sheet. The design method of the bandpass filter was derived by applying the equivalent network of the inductive strip to the usual method of the filter design such as shown in [2].

EQUIVALENT CIRCUIT OF INDUCTIVE STRIP

Fig. 1 shows the geometry and equivalent  $T$  network of the perfectly conductive strip inserted in a rectangular waveguide. In the cases of a short circuit and an open circuit at the central plane ( $T_0$ ) of the strip, the input admittances  $Y_1$  and  $Y_0$  were found, respectively;  $Z_s (\equiv jX_s)$  and  $Z_p (\equiv jX_p)$  in the equivalent  $T$  network of Fig. 1 (b) were easily calculated as follows:

$$Z_s = \frac{1}{Y_1} \tag{1}$$

$$Z_p = \frac{1}{2} \left( \frac{1}{Y_0} - \frac{1}{Y_1} \right) \tag{2}$$

From the Appendix, we have the following variational expression [3] for the normalized admittance  $y^{(i)}$ :

$$y^{(i)} = \frac{\sum_{n=3}^N Y_{0n} (\sum_{v=1}^N A_{vn} m_v)^2 + a \sum_{v=1}^N m_v^2 Y_v Q_v^{(i)}}{Y_{01} (\sum_{v=1}^N m_v A_{v1})^2} \tag{3}$$

where

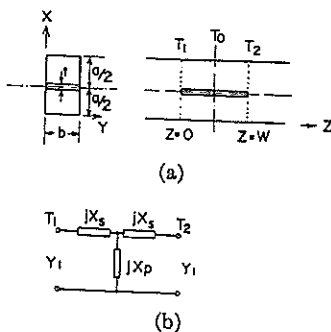
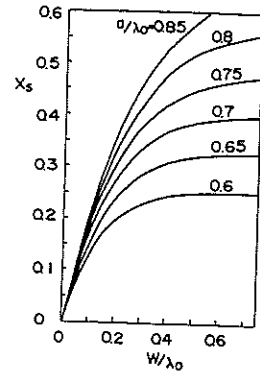
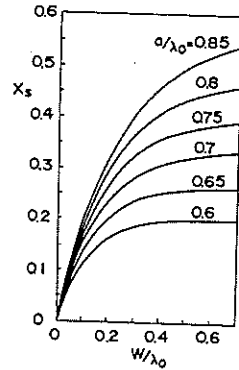


Fig. 1. Geometry and equivalent  $T$  network for an inductive strip. (a) Geometry. (b) Equivalent network.

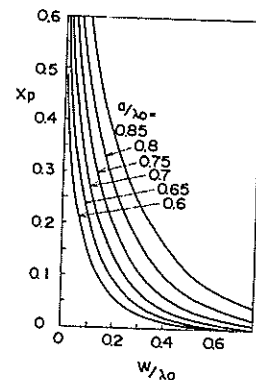


(a)

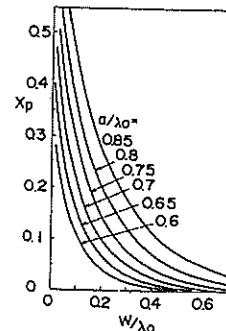


(b)

Fig. 2. Calculated values of normalized series reactance  $X_s$ . (a)  $t/\lambda_0 = 0$ . (b)  $t/\lambda_0 = 0.02$ .



(a)



(b)

Fig. 3. Calculated values of normalized shunt reactance  $X_p$ . (a)  $t/\lambda_0 = 0$ . (b)  $t/\lambda_0 = 0.02$ .

$$A_{vn} = (-1)^v \frac{8va^{1/2}}{\pi(n^2 - 4v^2)}$$

The case of  $i = 1$  gives an electric wall at  $Z = W/2$ , and  $i = 2$  gives a magnetic wall.

By the Rayleigh-Ritz method the amplitudes  $m_\nu$  are chosen so as to yield a minimum value of  $|y^{(i)}|$  for every  $\nu$ . The minimization conditions satisfy the following set of  $N - 1$  equations:

$$\frac{\partial y^{(i)}}{\partial m_j} = 0, \quad j = 2, 3, \dots, N \quad (4)$$

for  $m_1 = 1$ . Equation (3) was calculated by computer. Figs. 2 and 3 show the calculated values for the normalized series reactance  $x_s$  and the normalized shunt reactance  $x_p$ .

### DESIGN OF BANDPASS FILTER

The construction of the bandpass filter with inductive strips is shown in Fig. 4. Since the equivalent circuit of the strip is expressed with the inductive reactance  $T$  network as shown in Fig. 1, the equivalent circuit of the filter is given in Fig. 5(a). The symmetrical  $T$  reactance network connected to the transmission line operates as a  $K$ -inverter network [4] as shown in Fig. 6. Therefore, the equivalent circuit of Fig. 5(a) is transformed to Fig. 5(b).

Clearly, the phase constant  $\theta_j$  is given by

$$\theta_j = \frac{2\pi}{\lambda_0} l_j - \frac{1}{2}(\phi_j + \phi_{j+1}) \quad (5)$$

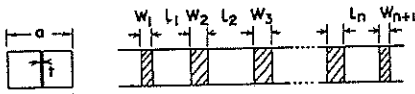


Fig. 4. Bandpass filter with inductive strip.

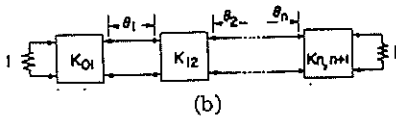
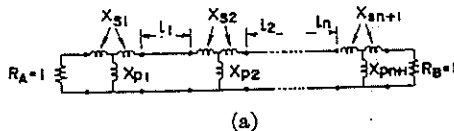
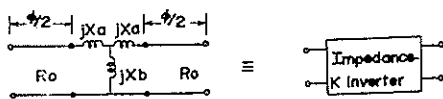


Fig. 5. Equivalent network. (a) Equivalent network. (b) Filter using impedance  $K$  inverter.

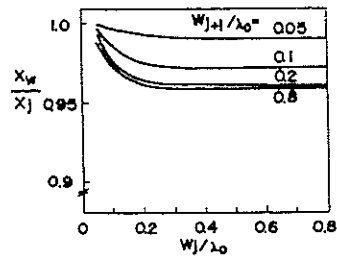


$$K = \left| \tan\left(\frac{\phi}{2} + \tan^{-1} Xa\right) \right|$$

$$\phi = -\tan^{-1}(2Xb + Xa) - \tan^{-1} Xa$$

in the case of  $Ro = 1$ .

Fig. 6. Impedance  $K$  inverter consisting of reactance  $T$  network and transmission lines.



$X_w = \frac{\pi}{2} \left( \frac{W_j}{\lambda_0} \right)^2$  Reactance slope parameter of half-wavelength waveguide (a)

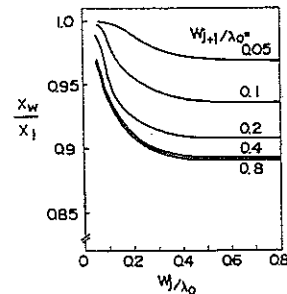


Fig. 7. Normalized reactance slope parameter. (a)  $a/\lambda_0 = 0.7$ ;  $t/\lambda_0 = 0.01$ . (b)  $a/\lambda_0 = 0.8$ ;  $t/\lambda_0 = 0.01$ .

where

$$\lambda_0 = \frac{\lambda_0}{[1 - (\lambda_0/2a)^2]^{1/2}}$$

$\theta_j$  ( $j = 1, 2, \dots, n$ ) is  $\pi$  at the center frequency by the design method of [2]. By the generalized equations for design of bandpass filters, we get the following relations:

$$X_j = \frac{\omega_0}{2} \frac{d\theta}{d\omega} \Big|_{\omega=\omega_0} \quad ; \text{reactance slope parameter} \quad (6)$$

$$\theta_j = \frac{2\pi}{\lambda_0} l_j - \frac{1}{2}(\phi_j + \phi_{j+1}) \quad (7)$$

$$\phi_j = -\tan^{-1}(2x_{pj} + x_{sj}) - \tan^{-1} x_{sj} \quad (8)$$

$$K_{j-1,j} = \left| \tan\left(\frac{1}{2}\phi_j + \tan^{-1} x_{sj}\right) \right| \quad (9)$$

$$K_{01} = \left( \frac{x_1 w}{g_0 g_1} \right)^{1/2} \quad K_{n,n+1} = \left( \frac{x_n w}{g_n g_{n+1}} \right)^{1/2}$$

$$K_{j,j+1} = w \left( \frac{x_j x_{j+1}}{g_j g_{j+1}} \right)^{1/2} \quad w = \frac{\Delta\omega}{\omega_0} \quad (10)$$

Fig. 7 shows the calculated values of  $x_j$ .

### DESIGN EXAMPLE FOR TWO-SECTION MAXIMUM FLAT FILTER

We will design the two-section maximum flat bandpass filter with the following specification:

center frequency  $\omega_0/2\pi = 10.9$  GHz

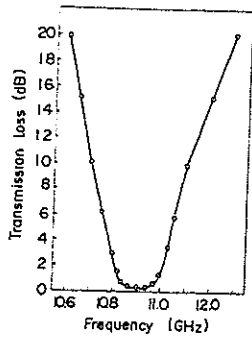


Fig. 8. Experimental response for two-section bandpass filter.

bandwidth	$\Delta\omega/2\pi = 218$ MHz
guide width	$a = 18.8$ mm
strip thickness	$t = 0.3$ mm.

The values calculated by the design method discussed in the previous section are as follows:

two strip widths	$W_1 = 2.4$ mm
	$W_2 = 8.2$ mm
distance between strips	$l = 15.5$ mm.

Fig. 8 is the transmission loss for the experimental bandpass filter. The experimental values of the filter produced by this design method are in good agreement with the specific values.

#### APPENDIX

Since the discontinuity is uniform along the  $y$  axis, the only types of higher order modes which are excited at the strip are  $H_{n0}$  modes. In the region  $Z \leq 0$ , the total transverse fields are given by the following expression:

$$E_y^{(i)} = a_1^{(i)} [\exp(-\Gamma_1 Z) + \gamma^{(i)} \exp(\Gamma_1 Z)] \phi_1 + \sum_n a_n^{(i)} \phi_n \exp(\Gamma_n Z) \quad (11)$$

$$H_x^{(i)} = -Y_{01} a_1^{(i)} [\exp(-\Gamma_1 Z) - \gamma^{(i)} \exp(\Gamma_1 Z)] \phi_1 + \sum_n Y_{0n} a_n^{(i)} \phi_n \exp(\Gamma_n Z), \quad n = 3, 5, 7, \dots \infty \quad (12)$$

where

$$\phi_n = \frac{2}{a^{1/2}} \sin \frac{n\pi x}{a} \quad (13)$$

$$Y_{0n} = \frac{\Gamma_n}{jk_0 \eta}, \quad n = 1, 3, 5, \dots \infty \quad (14)$$

$$\Gamma_n = \left[ \left( \frac{n\pi}{a} \right)^2 - k_0^2 \right]^{1/2}$$

$k_0 = 2\pi/\lambda_0 =$  wavenumber of free space

$\eta =$  characteristic impedance of free space.

The case of  $i = 1$  gives the electric wall at  $Z = W/2$ , and

$i = 2$  gives a magnetic wall. In the region  $0 \leq Z \leq W/2$ , it is assumed that all modes are evanescent.

Thus we get

$$E_y^{(i)} = \sum_m b_m^{(i)} \Psi_m A_m^{(i)}(Z) \quad (15)$$

$$H_x^{(i)} = \sum_m Y_m b_m^{(i)} \Psi_m B_m^{(i)}(Z), \quad m = 1, 2, 3, \dots \infty \quad (16)$$

where

$$A_m^{(1)} = B_m^{(2)} = \sinh T_m \left( Z - \frac{W}{2} \right)$$

$$A_m^{(2)} = B_m^{(1)} = \cosh T_m \left( Z - \frac{W}{2} \right)$$

$$\Psi_m = \frac{2}{(a-t)^{1/2}} \sin \frac{2m\pi x}{a-t} : \begin{cases} 0 \leq x \leq (a-t)/2 \\ (a+t)/2 \leq x \leq a \\ (a-t)/2 \leq x \leq (a+t)/2 \end{cases} = 0,$$

$$T_m = \left[ \left( \frac{2m\pi}{a-t} \right)^2 - k_0^2 \right]^{1/2}$$

$$Y_m = \frac{T_m}{jk_0 \eta}.$$

Since the transverse fields must be continuous at  $Z = 0$ , the following conditions are required:

$$\begin{aligned} \epsilon(x)^{(i)} &= a_1^{(i)} (1 + \gamma^{(i)}) \phi_1 + \sum_n a_n^{(i)} \phi_n \\ &= \sum_m b_m^{(i)} \psi_m A_m^{(i)}(0) \end{aligned} \quad (17)$$

$$\begin{aligned} Y_{01} a_1^{(i)} (\gamma^{(i)} - 1) \phi_1 + \sum_n Y_{0n} a_n^{(i)} \phi_n \\ = \sum_m Y_m b_m^{(i)} \Psi_m B_m^{(i)}(0). \end{aligned} \quad (18)$$

The coefficients  $a_n, b_m$  are expressible in terms of the electric field distribution  $\epsilon(x)$  as follows:

$$a_1^{(i)} = \frac{\int_0^{a/2} \epsilon^{(i)} \phi_1 dx}{1 + \gamma^{(i)}} \quad (19a)$$

$$a_n^{(i)} = \int_0^{a/2} \epsilon^{(i)} \phi_n dx, \quad (n = 3, 5, \dots \infty) \quad (19b)$$

$$a_n^{(i)} = \int_0^{(a-t)/2} \epsilon^{(i)} \Psi_m dx / A_m^{(i)}(0). \quad (19c)$$

Substituting the values of the coefficients into (18), we get

$$\begin{aligned} -Y_{01} \gamma^{(i)} \phi_1 \int_0^{a/2} \epsilon^{(i)} \phi_1 dx + \sum_n Y_{0n} \phi_n \int_0^{a/2} \epsilon^{(i)} \phi_n dx \\ = \sum_m Y_m \Psi_m \int_0^{(a-t)/2} \epsilon^{(i)} \Psi_m dx \cdot \frac{B_m^{(i)}(0)}{A_m^{(i)}(0)} \end{aligned} \quad (20)$$

where

$$y^{(i)} = \frac{1 - \gamma^{(i)}}{1 + \gamma^{(i)}} \quad (21)$$

$y^{(i)}$  is the normalized admittance at the plane  $Z = 0$ .

From (20), we have the following variational expression [3] for  $y^{(i)}$ :

$$y^{(i)} = \frac{\int_0^{a/2} \int_0^{a/2} G^{(i)}(x/x') \epsilon^{(i)}(x) \epsilon^{(i)}(x') dx dx'}{Y_{01} \left[ \int_0^{a/2} \epsilon^{(i)}(x) \phi_1 dx \right]^2} \quad (22)$$

where

$$G^{(i)} = \sum_{n=3} Y_{0n} \phi_n(x) \phi_n(x') + \sum_m Y_m Q_m^{(i)} \Psi_m(x) \Psi_m(x')$$

$$Q_m^{(1)} = \coth \frac{T_m W}{2}$$

$$Q_m^{(2)} = \tanh \frac{T_m W}{2}$$

The trial function  $\epsilon$  is given by

$$\epsilon = \sum_{\nu} m_{\nu} \sin \frac{2\nu\pi x}{a-t}, \quad \nu = 1, 2, 3, \dots, N. \quad (23)$$

Substituting (23) into (22), we get

$$y^{(i)} = \frac{\sum_{n=3} Y_{0n} (\sum_{\nu=1}^N A_{\nu n} m_{\nu})^2 + a \sum_{\nu=1}^N m_{\nu}^2 Y_{\nu} Q_{\nu}^{(i)}}{Y_{01} (\sum_{\nu=1}^N m_{\nu} A_{\nu 1})^2} \quad (24)$$

where

$$A_{\nu n} = (-1)^{\nu} \frac{S_{\nu} a^{1/2}}{\pi(n^2 - \nu^2)}$$

### REFERENCES

- [1] Y. Konishi *et al.*, "Simplified 12-GHz low-noise converter with mounted planar circuit in waveguide," *IEEE Trans. Microwave Theory Tech.* (Short Papers), vol. MTT-22, pp. 451-454, Apr. 1974.
- [2] G. L. Matthaei, L. Young, and E. M. T. Jones, *Microwave Filters, Impedance-Matching Network, and Coupling Structure*. New York: McGraw-Hill, 1964, p. 432.
- [3] R. E. Collin, *Field Theory of Guided Waves*. New York: McGraw-Hill, 1960, ch. 8.
- [4] G. L. Matthaei, L. Young, and E. M. T. Jones, *Microwave Filters, Impedance-Matching Network, and Coupling Structures*. New York: McGraw-Hill, 1964, p. 438.
- [5] Y. Konishi, "Microwave integrated circuits" (in Japanese), San-Po Co., Dec. 10, 1973.

# A Computerized Klinger Cavity Mode Conversion Test Set

BARRY S. SEIP AND LARRY W. HINDERKS

**Abstract**—A mode conversion test set utilizing the Klinger cavity technique has been developed for characterizing circular waveguide components in the millimeter waveguide region. The test set incorporates a precision linear displacement optical encoder and a specially designed controller which interfaces the test set to a Hewlett-Packard 2100 series computer. Control commands of a stored computer program are used by the operator for data acquisition and analysis. Experimental results show this system has high measurement accuracy and sensitivity while maintaining an uncomplicated measurement process.

### INTRODUCTION

**T**O MEET increasing communication needs, Bell Laboratories is engaged in developing a millimeter waveguide transmission system. This circular 60-mm-

diam waveguide uses the  $TE_{01}^{\circ}$  mode and operates from 40 to 110 GHz. It will have a capacity of approximately  $\frac{1}{4}$  million voice circuits.

In developing the waveguide system, measurement components are needed to transform the  $TE_{10}^{\square}$  mode into the  $TE_{01}^{\circ}$  mode in the 60-mm-diam waveguide. A combination of a transducer, mode filter, and helix taper is used to make the necessary transition from the millimeter wave source to the waveguide module being characterized. The  $TE_{01}^{\circ}$  mode launching components are used in determining the  $TE_{01}^{\circ}$  mode transmission characteristics of the waveguide modules.  $TE_{11}^{\circ}$  and  $TE_{12}^{\circ}$  mode launchers have been designed for determining the unwanted mode attenuation of waveguide modules. The modal purity of all transducers and tapers must be known before they can be reliably used in test sets. The Klinger cavity method [1] is a powerful method for determining modal purity.

Manuscript received May 3, 1973; revised April 29, 1974.  
The authors are with Bell Laboratories, Inc., Murray Hill, N. J. 07974.